

Modeling and Experimental Study on Grid-Connected Inverter for Direct Drive Wind Turbine

HUANG Wang-jun^{*1}, ZENG Zhi-gang¹, ZHOU Hui-fang², TEN Yuan-jiang³, Li Li¹

¹College of Elect. and Information, Hunan Institute of Engineering, Xiangtan 411101, China;

²Department of Elect. and Information, Hunan Electrical College of Technology, Xiangtan 411101, China;

³College of Mathematical and Physics, Hunan Institute of Engineering, Xiangtan 411101, China;

Shuyuan Road No. 17 Xiangtan, Hunan, China. 073158688933/073158688933

*Corresponding author, e-mail: hwj8423@sina.com

Abstract

This paper designs a dual topological structure of grid-connected inverter for high-power wind turbine, introduces PWM converter's operational state, and establishes its mathematical model, then it puts forward the dual closed-loop vector control strategy of grid-side converter based on dq coordinate. The combination of the dual topological structure and decoupling control realizes the functioning of high-power factor and two-way transmission of energy. Grid-side converter can stabilize DC side voltage and adjust active or reactive output current independently when wind velocity changes rapidly, which leads to the change of output power in generator. The hardware experiment and simulation results verify the feasibility of the proposed control scheme in both the high stability accuracy and excellent property of grid-connection.

Key Words: direct drive wind turbine, grid-side converter, dq coordinate, vector control, PWM

Copyright © 2013 Universitas Ahmad Dahlan. All rights reserved.

1. Introduction

Direct drive system has been one of main trends in wind power generation field because of its low cost, less noise & better ability of low voltage ride through (LVRT) [1-2]. The control method of variable speed constant frequency (VSCF) is always taken in the high-power wind power generation system for its maximum wind energy extraction [3-4].

At present, there are two ways of VSCF. One is the comparatively maturer theory of using grid-connected doubly-fed generator system, which is mainly based on the decoupling control of active & reactive powers of stator flux doubly-fed turbine, and on the grid-connected control method of voltage oriented vector as well. In this case, however, it is difficult to manufacture and maintain the generators. Another is MW class permanent magnet direct drive generator grid connection system. The research on it has just started at home. In recent years, the operation and power quality of the system controlled by double PWM has been focused on. The theoretical research and simulation of converters using parallel dual structure has also been realized [7]. The performance of converters greatly depends on the AC control, and more researches of the PWM converter control method have been achieved [8-15]. Currently such control ways as PI, hysteresis control and proportional resonance control are commonly used. The conventional PI control can only eliminate the steady-state error of DC reference signal, thus it is difficult to track the AC components in given value without difference. The hysteresis control is characterized by simple circuit and quick dynamic response. But the hysteresis width influences the switch frequency, loss and control accuracy. Zero steady-state error can be achieved when the proportional resonance control gain in fundamental frequency is infinite in the case of AC [16-17].

This paper, on the basis of the dual topological structure and dq coordinate, designs a dual closed-loop vector control strategy in the high-power wind turbine, establishes its mathematical model of grid-side converter, and verifies it through hardware experiments and simulation. The results can guide the design and industrialization of grid-connected inverter for direct drive wind turbine.

2. Dual Topological Structure

The structure of wind turbine grid-connected inverter is shown in Figure 1. C1 and C2, DC bus support capacities, can serve to stable dc bus voltage and constitute a voltage source PWM inverter circuit. LC composes filter circuit, and effectively filters the high harmonic produced by grid-connection. Between the machine side converter and web side converter, a brake unit, composed of T1, T2 and R1, is designed to protect the device once the grid voltage drops or the power is suddenly cut off.

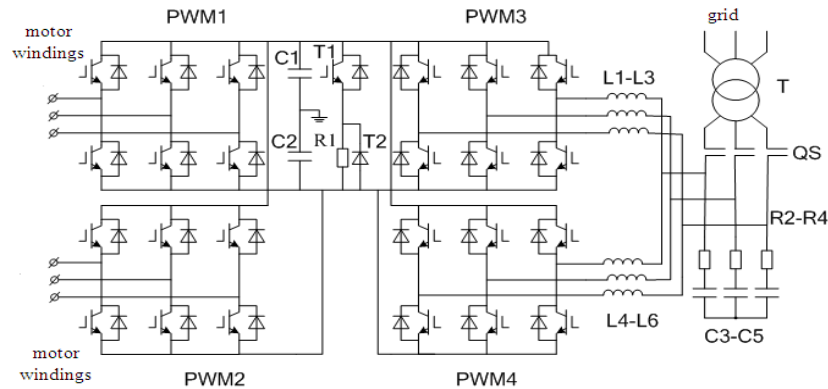


Figure 1. Structure Diagram of Wind Turbine Grid-Connected Inverter

The whole system consists of four symmetrical PWM modules. PWM1 and PWM2 compose the machine-side converter, while PWM3 and PWM4 compose the grid-side converter. The machine-side and grid-side converter modules share the same DC bus. To improve the equivalent switching frequency and reduce the capacity of filter reactor, thus to improve the system stability, the phase difference of carriers between the two three-phase whole-bridge PWM inverter circuit must be controlled to make it work in the dual model.

3. Working State and Controlling Strategy of the Converter

3.1. Working State

The machine-side and grid-side converters are connected in a back-to-back mode. Thus the frequency & amplitude conversion value power of permanent magnet generator can be transformed into active and reactive power to adjust constant frequency electric parameters of grid-connection independently [1]. In the wind power grid system, because of the power bidirectional transmission, PWM converters operate in the rectification working state when getting energy from the grid, and the grid-side voltage is in phase with current (positive resistance characteristic). And when the PWM converters transmit power to the grid, they operate in the active inverter working state, and the grid-side voltage is out of phase with current (negative resistance characteristic). To realize the PWM converters operation in the forth quadrant, the key lies in controlling grid-side current.

3.2. The Mathematical Modeling of the Grid-side Converters

Three coordinate systems, namely three-phase static coordinate system (abc), two-phase stationary coordinate system ($\alpha\beta$) and two-phase rotating coordinate system (dq) are defined in the study of vector controlling. The matrix transformation is achieved under the equal power coordinate transformation at first [11,13]. The transformation matrix from three-phase static coordinate system to the two-phase vertical rotating coordinate system is as shown in (1).

$$\begin{bmatrix} x_d \\ x_q \end{bmatrix} = \sqrt{\frac{2}{3}} \begin{bmatrix} \cos\theta & \cos(\theta - \pi/3) & \cos(\theta + \pi/3) \\ -\sin\theta & -\sin(\theta - \pi/3) & -\sin(\theta + \pi/3) \end{bmatrix} \begin{bmatrix} x_a \\ x_b \\ x_c \end{bmatrix} \quad (1)$$

In order to facilitate the building of the model, the same point is selected as both the AC-side voltage reference point and grid voltage reference point, which can be seen as the point 0 in Figure 2.

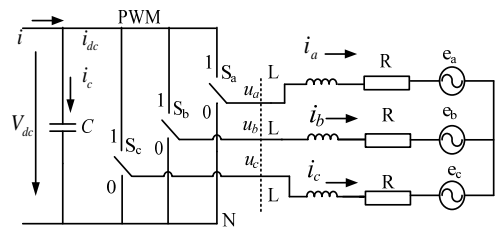


Figure 2. Main Circuit of PWM Inverter

The relation between PWM converter AC voltage and current is shown as (2).

$$\begin{bmatrix} u_a \\ u_b \\ u_c \end{bmatrix} = L \begin{bmatrix} \frac{di_a}{dt} \\ \frac{di_b}{dt} \\ \frac{di_c}{dt} \end{bmatrix} + R \begin{bmatrix} i_a \\ i_b \\ i_c \end{bmatrix} + \begin{bmatrix} e_a \\ e_b \\ e_c \end{bmatrix} \tag{2}$$

After the zero axis component being added, (1) is inversely transformed. Then it is substituted into (2), and the zero axis component is omitted from the result. The result is:

$$\begin{bmatrix} u_d \\ u_q \end{bmatrix} = L \begin{bmatrix} \frac{di_d}{dt} \\ \frac{di_q}{dt} \end{bmatrix} - \begin{bmatrix} 0 & \omega L \\ -\omega L & 0 \end{bmatrix} \begin{bmatrix} i_d \\ i_q \end{bmatrix} + R \begin{bmatrix} i_d \\ i_q \end{bmatrix} + \begin{bmatrix} e_d \\ e_q \end{bmatrix} \tag{3}$$

In the same way, relationship between DC side voltage and current can be got as follows:

$$C \frac{dU_{dc}}{dt} = i - \begin{bmatrix} S_a & S_b & S_c \end{bmatrix} \begin{bmatrix} i_a \\ i_b \\ i_c \end{bmatrix} \tag{4}$$

In the formula, S_a, S_b, S_c are switch functions. To build the PWM converter mathematical model based on the switching function, (4) is transformed into dq coordinate system,

$$C \frac{dU_{dc}}{dt} = i - S_d i_d - S_q i_q \tag{5}$$

Under the balanced three-phase power grid, the inductance of the equivalent resistance R is ignored, employing feed-forward decoupling control strategy, the PWM converter input voltage can be got according to (6), and the current PI controller can accordingly be designed, too.

$$\begin{cases} u_d = (K_p + \frac{K_I}{S})(i_{dref} - i_d) - \omega L i_q + e_d \\ u_q = (K_p + \frac{K_I}{S})(i_{qref} - i_q) + \omega L i_d + e_q \end{cases} \tag{6}$$

In the dq coordinate system, the active and reactive powers of the three-phase grid-connection PWM converter are:

$$\begin{cases} P = e_d i_d + e_q i_q \\ Q = e_d i_q + e_q i_d \end{cases} \quad (7)$$

In the stable state, the average of the q axis is zero, so

$$\begin{cases} P = e_d i_d \\ Q = e_d i_q \end{cases} \quad (8)$$

From (8) we can get the conclusion that in the q axis, as long as the active current i_d and reactive current i_q are controlled effectively and independently, the independent decoupling control of the active and reactive outputting powers of the converter can be completely achieved.

4. Control Strategy of Grid-Side Converter

To achieve the system's unit power factor operation in rectifying and inverting conditions, keeping constant DC voltage of the grid-side converter, and minimum influence on the converter & grid while being connected to grid, double closed-loop vector control strategy is adopted. In dual topology, each inverter is controlled by individual independent command current, and the structure of each control module is shown as in Figure 3.

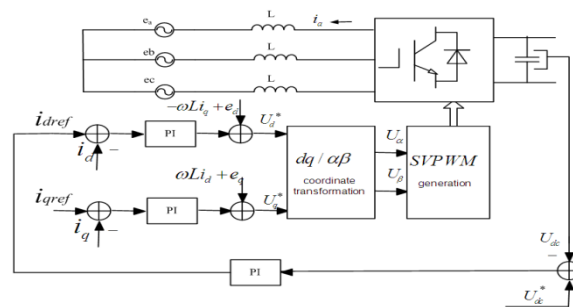


Figure 3. Converter Control Module

As is shown in Figure 3 in the double closed-loop structure, PI control in the outer voltage ring is to stable DC bus voltage and give inner current ring instruction. PI control in the inner current ring is to, based on the output current instruction from the outer voltage ring, control the current to achieve the unit power factor, reactive power compensation and so on. SVPWM modulation in the grid-side converter is to improve the utilization rate of DC voltage and dynamic characteristics.

4.1. The Inner Current Ring Controller

The response of the current loop affects not only the control of AC-side current waveform and power factor, but also the ability of tracking DC-side voltage and the immunity of the system when the power changes. The type and parameter of the inner controller are the greatest impact factors on the performance of the current loop. Therefore, the inner current ring is designed according to the typical Type II in the system.

Based on the dq model of grid-connection converter, the current instruction of the three-phase control is determined according to (7). The decoupling control structure in the inner current ring is shown as Figure 4.

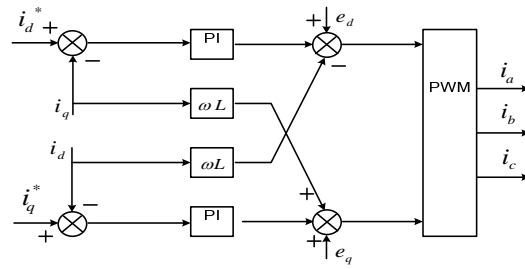


Figure 4. The Decoupling Control Structure in Current Inner Ring

Considering the signal sampling delay of the inner current ring and the slight inertia of PWM control, the inner ring structure of the decoupled i_d current is shown as Figure 5.

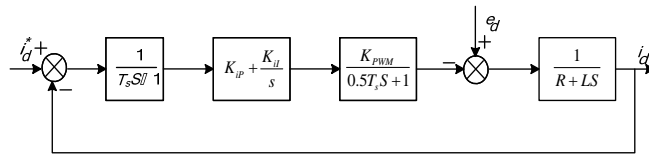


Figure 5. Inner i_d Ring Structure

In Figure 5, T_s is the current sampling period (i.e the PWM switch cycle) of the inner current ring, and e_d is disturbance quantity. The inner current ring control structure is shown as Figure 6 when the AC-side resistance is ignored.

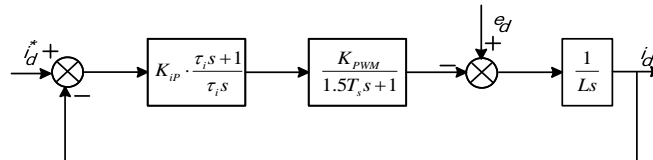


Figure 6. Simplified Structure of Inner i_d Ring when e_d is Disturbed

Its open-loop transmission function is:

$$W_{oi}(s) = \frac{K_{ip} K_{PWM}}{\tau_i L} \cdot \frac{\tau_i s + 1}{s^2 (1.5 T_s s + 1)} \tag{9}$$

To improve the current response rapidity, appropriate medium frequency, h_i [$h_i = \tau_{i/1.5} T_s$], can be designed in Type II system ($h_i = 5$ is often adopted in projects). According to the parameter design relationship in Type II system, we get:

$$K_{ip} = \frac{(h_i + 1)L}{2\tau_i K_{PWM}} = \frac{6L}{15T_s K_{PWM}} \tag{10}$$

$$K_{il} = \frac{K_{iP}}{\tau_i} = \frac{6L}{112.5T_s^2 K_{PWM}} \quad (11)$$

As Equation (10) & (11) shown, the inner current ring can be approximately equivalent to an inertial link, and its inertial time constant is $3T_s$. When the switching frequency is high enough, faster dynamic response of the inner current ring can be achieved.

4.2 Design of the Outer Voltage Ring Controller

The purpose of the outer voltage ring is to control the constant DC bus voltage of grid-side inverter to reduce the interference with the grid-side AC current to improve power quality and voltage protection of power devices as well. The control structure of the outer voltage ring is designed as Figure 7,

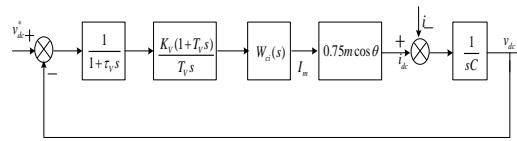


Figure 7. Control Structure of Outer Voltage Ring

According to Type II, the open-loop transmission function of voltage ring is:

$$W_{ov}(s) = \frac{0.75 K_v (T_v s + 1)}{C T_v s^2 (T_{ev} s + 1)} \quad (12)$$

According to the setting relationship of the control parameters in Type II, we get:

$$\frac{0.75 K_v}{C T_v} = \frac{h_v + 1}{2 h_v^2 T_{ev}^2} \quad (13)$$

The medium frequency width $h_v = T_v / T_{ev} = 5$ being taken,

$$\begin{cases} T_v = 5T_{ev} = 5(\tau_v + 3T_s) \\ K_v = \frac{4C}{5(\tau_v + 3T_s)} \end{cases} \quad (14)$$

And the cutoff frequency of the voltage loop control system is:

$$\omega_c = \frac{1}{2} \left(\frac{1}{T_v} + \frac{1}{T_{ev}} \right) \quad (15)$$

So the bandwidth of the voltage loop is:

$$f_{bv} \approx \frac{\omega_c}{2\pi} = \frac{3}{20T_s \times 2\pi} \approx 0.024 f_s \quad (16)$$

where f_s is the PWM switching frequency.

5. Simulation Research

In order to better verify the controlling strategy, MATLAB is employed to simulate 10kVA grid-side converter, where 620V DC voltage, 380V AC voltage, 50Hz grid frequency, 2mH AC-side inductance, and 4700 μ F DC bus capacity are adopted.

The a-phase voltage and current waveforms are shown as Figure 8. It shows that the grid voltage and current are in phase and unit power factor grid-connection is realized to reduce the harmonic content of the grid-connection current.

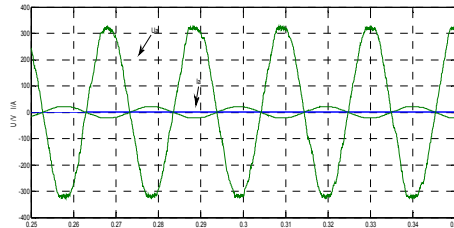


Figure 8. A-phase Voltage and Current Waveforms

When the current step response is given and the grid-connection current i_d^* steps from 22A to 44A in 0.2s, the dynamic response of the grid current is shown as Figure 9. It shows that under the step condition, current tracks rapidly, while the overshoot is very small and a reliably response can be completed in a power frequency cycle.

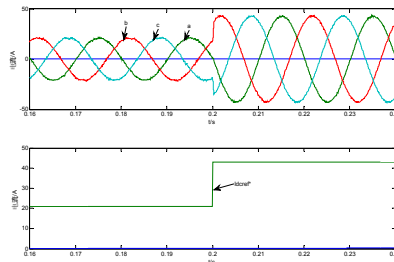


Figure 9. Dynamic Response Waveforms of Grid Current

6. Experimental Verification

By using TMS320F2812 as the control core, an experimental system is built according to the Figure 1 and a grid-side stabilivolt experiment system is designed to test the grid-connection characteristics of the device. A outer voltage ring is added to the experiment debugging of the current closed-loop control and the grid-side converter is connected to grid through the connection transformer to stable DC voltage. 380V AC line voltage and 750V DC are adopted. Steady-state DC bus voltage waveform is shown as Fig.10. It shows that the stability effect of the double closed-loop voltage is evident and the precision of the DC stabilivolt is high.



Figure 10. Waveform of Stabilivolt

The grid-connection field test of the wind turbine is simulated where 380V AC grid is connected on one side and 6-phase permanent magnet synchronous motor is on another side. Waveforms of the AC-side voltage (the large amplitude), the AC-side current (the small amplitude) and DC-side voltage (the horizontal wave) is shown as Figure 11. The experiment results show that the permanent magnet motor can be connected smoothly with the grid.

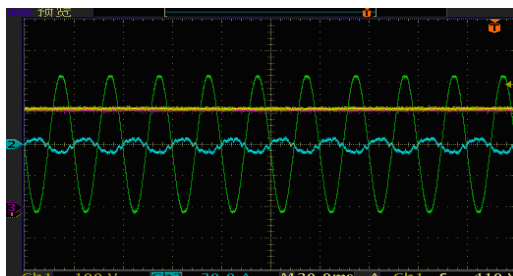


Figure 11. Waveforms of AC-side Voltage and Current and DC-side Voltage

To prevent the short-circuit problem existing in the same bridge arm, certain dead-time must be set, which is tested as in Figure 12. The dead-time is set as $3.5\mu\text{s}$.

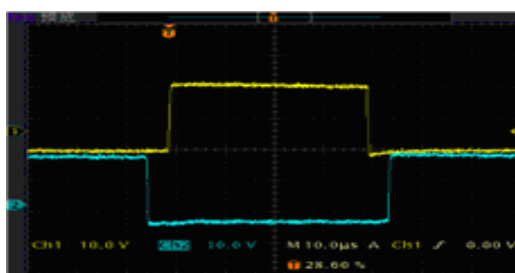


Figure 12. Dead-time Testing

7. Conclusion

Based on the dual topological structure of grid-connected inverter for high-power wind turbine and dq coordinate, in this paper double closed-loop vector control strategy of permanent magnet direct-drive wind turbines is introduced, the grid-side mathematical model of the converter is established, its simulation verification & experimental research are accomplished. The results show that under high power factor and constant DC bus voltage the converter can operate with higher stability accuracy and immunity. The success of a prototype is of practical engineering value and lays the foundation for grid-connection device industry.

References

- [1] FU Xunbo, GUO Jindong, ZHAO Dongli, et al. Characteristics and simulation model of direct-drive wind power system. *Electric Power Automation Equipment*. 2009; 29(2): 1-5.
- [2] HU Wei-hao, WANG Yue, LI Ming, WANG Zhao-an. Modeling and Control of a novel Experimental Method for High Power Wind Power Converter. *Power Electronics*. 2009; 43(10): 14-15.
- [3] ZHANG Jin-song, LIU Lian-gen, XU Feng-xing, SHE Yue. Principle Analysis of Connected-Grid Control Method for Doubly-fed Wind Power Generator and Its Simulating Experimental Research. *High Power Converter Technology*. 2010; 3: 38-41.
- [4] Zhou Peng, He Yikang, Hu Jiabing. Detection of Voltage Synchronization Signals for a Wind Energy Generation System Unbalanced Grid Conditions. *Transactions of China Electrotechnical Society*, 2008; 23(5): 108-113.
- [5] He Yikang, Hu Jiabing. The Imitation Of Wind Turbine Characteristic Using Dcmotor In Neration. *Acta Energiæ Solaris Sinica*. 2006; 27(10): 1006-1013.

- [6] CHEN Wei, CHEN Cheng, SONG Zhan-feng, XIA Chang-liang. *Proportional-resonant Control for Dual PWM Converter in Doubly Fed Wind Generation System*. Proceedings of the CSEE. 2009; 29(15): 1-7.
- [7] Zhou Jinghua, Su Yanmin, Zhan Xiong. A Control Scheme for Multi-cell-cascade High-power Inverter. *Electric transmission*. 2004; 34(1): 39-41.
- [8] Xiong Jian, Zhou Liang, Zhang Kai, Shi Pengfei. A High Precision Multi-Loop Control Strategy for Single-Phase PWM Inverters. *Transactions of China Electrotechnical Society*. 2006; 21(12): 79-83.
- [9] OUYANG Hong-lin, CHEN Ji-hua, HUANG Shou-dao, et al. Investigation of an Improved Control Strategy for Three-Phase PWM Voltage Rectifier. *Journal of Hunan University*. 2005; 32(3): 93-96.
- [10] ZHOU La-wu, XU Yong, ZHU Ying-hao. Simulation of PWM Reactor Based Static Var Compensator. *Journal of Hunan University (Natural Sciences)*. 2003; 30(4): 58-61.
- [11] YU Jing-rong, ZHANG Jing. A New Dead-beat Current Control Method for Active Power Filter Based on Voltage Space Vector. *Journal of Hunan University (Natural Sciences)*. 2008; 35(10): 31-35.
- [12] Fukuda S, Yoda T. A Novel Current-tracking Method for Active Filters Based on a Sinusoidal Internal Mode. *IEEE Trans on Industry Applications*. 2001; 37(3): 888-895.
- [13] Jiang Junfeng, Liu Huijin, Chen Yunping, et. al. *A novel double hysteresis current control method of active power filter with voltage space vector*. Proceedings of the CSEE. 2004; 24(10): 82-86.
- [14] ZHAO Qing-lin, GUO Xiao-qiang, WU Wei-yang. *Research on Control Strategy for Single-phase Grid-connected Inverter*. Proceedings of the CSEE. 2007; 27(16): 60-64.
- [15] JIANG Jun-feng, LIU Hui-jin, CHEN Yun-ping, et al. *A Novel Double Hysteresis Current Control Method of Active Power Filter with Voltage Space Vector*. Proceedings of the CSEE. 2004; 24(10): 82-86.
- [16] TU Chun-ming, LUO An, TANG Ci, et al. *Control of Injection Type Hybrid Active Power Filter*. Proceedings of the CSEE. 2008; 28(24): 52-57.
- [17] Ali Mohammadi, Sajjad Farajianpour .etc. Fluctuations Mitigation of Variable Speed Wind Turbine Through Optimized centralized Centralized Controller. *Telkomnika*. 2012; 10(4): 659-669.
- [18] Huang wangjun. Modeling and Simulation Research on Lightning Over-voltage of 500kV Hydroelectric Station. *Telkomnika*. 2012; 10(4): 619-624.
- [19] LI Li, ZHAO Kui-yin1, XU Xin-yuan, ZHU Jian-lin. Study on control strategy of a proportional-resonant control scheme with feed-forward compensator for the single-phase PWM rectifier. *Power System Protection and Control*; 2010; 38(9): 75- 79.